THE JOURNAL OF PHYSICAL CHEMISTRY Letters

Letter

pubs.acs.org/JPCL

Rabi Splitting in Photoluminescence Spectra of Hybrid Systems of Gold Nanorods and J-Aggregates

Dzmitry Melnikau,[†] Ruben Esteban,[*,‡] Diana Savateeva,[†] Ana Sánchez-Iglesias,[§] Marek Grzelczak,[§] Mikolaj K. Schmidt,[†] Luis M. Liz-Marzán,[§,∥] Javier Aizpurua,[†,‡] and Yury P. Rakovich[*,†,‡,∥]

[†]Centro de Física de Materiales (MPC, CSIC-UPV/EHU), Paseo Manuel de Lardizabal 5, Donostia-San Sebastián 20018, Spain

[‡]Donostia International Physics Center (DIPC), Paseo Manuel de Lardizabal 4, Donostia-San Sebastián 20018, Spain

[§]CIC biomaGUNE, Paseo de Miramon 182, Donostia-San Sebastián 20009, Spain

[∥]IKERBASQUE, Basque Foundation for Science, Maria Diaz de Haro 3, Bilbao 48013, Spain

Supporting Information

ABSTRACT: We experimentally and theoretically investigate the interactions between localized plasmons in gold nanorods and excitons in J-aggregates under ambient conditions. Thanks to our sample preparation procedure we are able to track a clear anticrossing behavior of the hybridized modes not only in the extinction but also in the photoluminescence (PL) spectra of this hybrid system. Notably, while previous studies often found the PL signal to be dominated by a single mode (emission from so-called lower polariton branch), here we follow the evolution of the two PL peaks as the plasmon energy is detuned from the excitonic resonance. Both the extinction and PL results are in good agreement with the theoretical predictions obtained for a model that assumes two interacting modes with a ratio between the coupling strength and the plasmonic losses close to 0.4, indicative of the strong coupling regime with a significant Rabi splitting estimated to be ~200 meV. The evolution of the PL line shape as the plasmon is detuned depends on the illumination wavelength, which we attribute to an incoherent excitation given by decay processes in either the metallic rods or the J-aggregates.

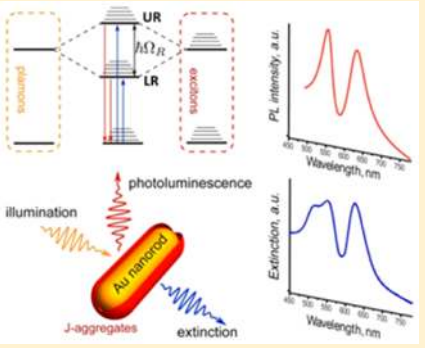

One of the main objectives of nanophotonics research is the control of the light−matter interaction on the nanoscale. The coupling between plasmonic and excitonic resonances (plexitonic coupling)[1−4] is of great interest in fundamental studies and for many practical applications in integrated optics, optoelectronics, imaging, and sensing.[5,6] The interaction between plasmons and excitons strongly affects energy and electron-transfer pathways[7] and, as a result, absorption and emission properties.[8] Especially attractive for many applications is the so-called strong coupling regime, produced when the rate of coherent energy exchange between the excitonic and plasmonic systems exceeds the rate of the losses in the system.[5] If both the excitons and the plasmon modes are modeled as coupled harmonic oscillators, the energies of the new hybrid plexcitonic modes are given by[9,10]

$$E_{\pm} = \frac{\hbar}{2}\left[\omega_{pl} + \omega_{ex} - i\left(\frac{\kappa}{2} + \frac{\gamma_s}{2} + \gamma_d\right)\right] \pm \frac{\hbar}{2}\sqrt{4|g|^2 + \left[\delta + i\left(\frac{\gamma_s}{2} + \gamma_d - \frac{\kappa}{2}\right)\right]^2} \quad (1)$$

where g is the interaction coupling strength between the two oscillators, ω_{pl} and ω_{ex} are the angular frequencies of the plasmonic and excitonic excitations, respectively, and $\delta = \omega_{pl} - \omega_{ex}$ is the detuning. The losses are described by the plasmonic damping κ of the metallic nanoparticle and the spontaneous decay γ_s and pure dephasing γ_d rates of the emitter. For sufficiently low losses, these new eigenstates with energies E_+ and E_- spectrally reveal themselves as the upper (UR) and lower (LR) resonant peaks, respectively, that anticross as $\delta \to 0$. When the exciton resonance energy matches the plasmonic band energy ($\delta = 0$), the term $Re(E_+ - E_-)$ (where Re indicates the real part) gives the energy of the Rabi splitting $\hbar\Omega_R = Re(E_+ - E_-)$. The onset of the strong coupling regime can be identified by the positive value of the Rabi splitting $\hbar\Omega_R > 0$ defined by eq 1, which for negligible losses reaches $\Omega_R = 2|g|$. A more demanding condition requires Ω_R to be at least comparable to the losses, so that the separation between the two modes is not much smaller than their width.[11] The strong coupling regime can also be identified by the emergence of Rabi oscillations in the time evolution, as recently demonstrated for several plasmonic systems.[12,13]

One of the advantages of plasmonic structures is the extremely low modal volume associated with their electromagnetic resonances, one of the prerequisites for achieving strong coupling strengths, g; however, because of the very fast

Received: November 10, 2015
Accepted: January 2, 2016

DOI: 10.1021/acs.jpclett.5b02512
J. Phys. Chem. Lett. 2016, 7, 354−362

decay rates of plasmons, it still remains very challenging to achieve strong coupling $\hbar\Omega_R > 0$ for single molecules or quantum dots with moderate oscillator strengths.[14−16] In this respect, coupling the plasmons with excitons of organic dyes in the J-aggregated state is of significant interest for the development of advanced photonic technologies based on organic−inorganic hybrid nanosystems. This is due to the ability of J-aggregates to delocalize and migrate excitonic energy over a large number of aggregated dye molecules, which results in an extremely high oscillator strength.[17] Other organic molecules have also been used in previous studies.[18,19]

While observation of Rabi splitting in extinction or transmission spectra of plexitonic structures that combine metal nanoparticles and J-aggregates has been reported in a number of publications (Supporting Information S1[1,20−26] and S2[27−39]), photoluminescence (PL) properties of a plexitonic hybrid system in the strong coupling regime are more elusive to experimental investigation.[36,39] Treating the system as two simple coupled modes leads to a Rabi splitting in both the extinction spectra and the PL,[40,41] but observing the latter can be hindered by other phenomena, as, for example, changes in the dynamics of the energy transfer and recombination processes between the levels of the complex electronic structure of the J-aggregates involving vibrational sublevels,[42] defect states in J-aggregate systems, and sometimes the presence of incoherent (uncoupled or undressed) states in coupled systems.[36] These might be the reasons why observation of emission from both UR and LR branches in PL spectra of plexitonic nanostructures has, to the best of our knowledge, not yet been reported.

In this study we identify Rabi splitting in PL spectra by investigating the strong exciton−plasmon interaction in a system consisting of J-aggregates of cyanine dye and gold nanorods. We first estimate the Rabi splitting at zero detuning from the anticrossing behavior of the bands in extinction spectra. To that end the resonant wavelength of the nanorods is tuned to control the spectral overlap between the exciton and plasmon bands. We obtain an Ω_R value similar to the largest splittings observed in planar organic microcavities or in plexitonic systems based on gold particles. Next, we focus on the signature of the strong coupling in the evolution of the PL modes, which we can identify due to the pronounced emission from both the UR and LR branches. The evolution of the modes is consistent with the results from the extinction, which corroborates the interpretation of the modes in terms of an anticrossing. We further use a theoretical model of emission to analyze the PL spectra and discuss their dependence on the excitation wavelength.

Gold nanorods (65.5 nm × 14.9 nm - sample g in Figure 1; see also Supporting Information S3 and S4) were prepared using Ag-assisted seeded growth,[43] and subsequently partially oxidized[44] to obtain nanorods with desirable aspect ratio (Supporting Information S3) and position of the plasmon bands (Supporting Information S4). In this way nanorods of similar diameter (in the range of 15−18 nm) but of different lengths (from 34 to 65.5 nm) were specifically synthesized to study exciton/plasmon coupling as a function of detuning with respect to the position of the J-band in the extinction spectrum of JC-1 dye J-aggregates. TEM imaging of nanorods presented in Figure 1 confirms the nanoparticles dimensions.

Using the poor solubility of the selected cyanine dye in water and its ability to form J-aggregates in a medium of high polarity, we produced hybrid structures of gold nanorods and J-aggregates by injection of the concentrated ethanol solution of the dye into an aqueous solution of gold nanorods in the presence of ammonia (see Methods). The main mechanism of the formation of the hybrid system is assumed to be electrostatic interactions between the cationic sites of hexadecyltrimethylammonium bromide (which is the agent stabilizing the surface of Au nanorods) and anionic groups of the J-aggregates.[20] The formation of the hybrid structures has been further confirmed by surface-enhanced Raman scattering (Figure 1h) as the hot spots provided by Au nanorods are expected to enhance the Raman scattering response of the attached organic compounds.

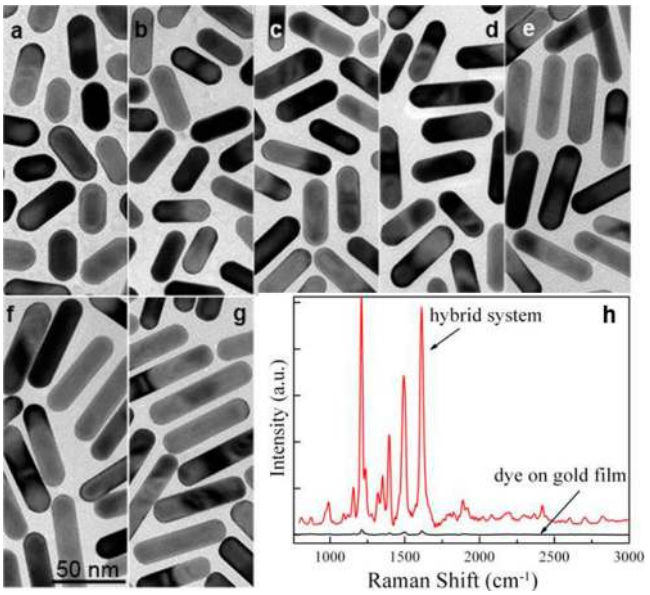

Figure 1. (a−g) TEM images of gold nanorods with different aspect ratios and (h) representative surface-enhanced Raman spectrum of the hybrid nanostructure of gold nanorods (sample c) and the J-aggregates of JC-1 dye (red line) in comparison with Raman spectrum of JC-1 dye on a gold film (black line). The PL background was subtracted in both spectra in panel h. The scale bar in panel f is valid for all samples (a−g).

Gold nanorods exhibit at least two plasmon resonances, a transverse mode (TM) due to the oscillation of the electrons perpendicular to the long axis of the rod, and a dipolar longitudinal mode (LM) caused by oscillations along the axis. The latter depends almost linearly on the aspect ratio, and it is widely tunable in the visible and in the near-infrared region of the spectrum (from 598 to 855 nm in our case, Figure 2a). On the other hand, J-aggregates, having extremely high oscillator strength,[17] show a very narrow extinction band (J-band) centered around 592 nm with a full width at half-maximum (fwhm) of 8 nm. The absorption band of dye monomers is much broader and positioned at 505 nm. Both peaks are observed in the spectrum presented in Figure 2c, which was measured in the absence of nanorods. The possibility to tune the plasmonic resonance from close proximity to the J-band to large spectral separation is a key factor behind our choice of dye and plasmon structures, allowing us to investigate how the hybridized modes evolve as a function of the detuning δ.

Figure 2b shows the extinction spectra of the hybrid plasmon-exciton system formed using the nanorods of various aspect ratios spectrally characterized in Figure 2a. The weak peak near 500 nm is related to the nanorods TM plasmon resonance, whose spectral position remains unaffected by the

DOI: 10.1021/acs.jpclett.5b02512
J. Phys. Chem. Lett. 2016, 7, 354−362

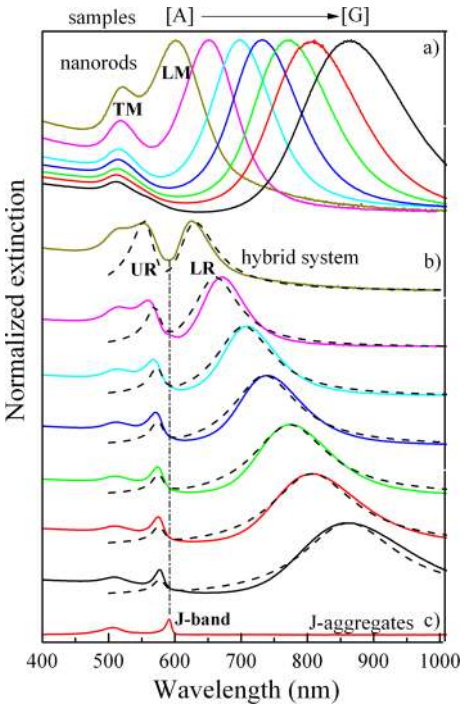

Figure 2. Experimental (solid lines) and simulated (dashed lines) normalized extinction spectra of (a) gold nanorods with different aspect ratio, (b) hybrid J-aggregates/gold nanorods complexes, and (c) spectrum of pure J-aggregates measured in the absence of nanorods. In panel a, samples A−G correspond, respectively, to panels a−g in Figure 1, and the peaks are centered at 597.8, 646.3, 692.3, 725.2, 763.9, 798.3, and 854.4 nm. In panel b, the different spectra are vertically shifted for clarity and the upper traces correspond to smaller detunings δ, found for lower aspect ratios of the rods in Figure 1. Vertical dashed-dotted line indicates the spectral position of the J-band. The theoretical spectra use $g/\kappa = -0.4i$.

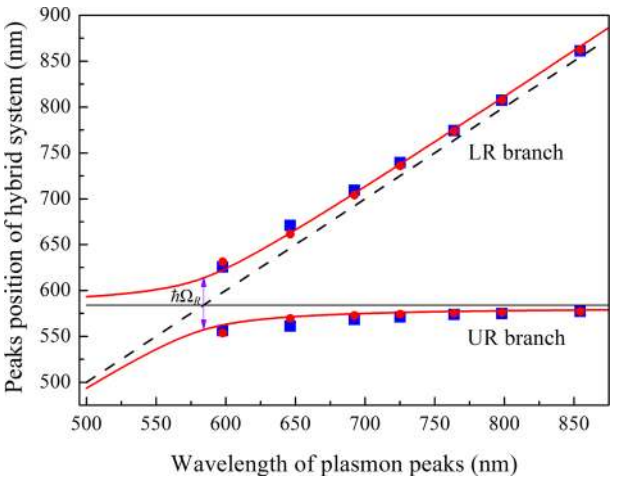

Figure 3. Results of the theoretical analysis of the peak positions in the extinction spectra obtained for $g/\kappa = -0.4i$ (red circles) in comparison with the experimental data (blue squares). The horizontal solid line indicates the spectral position of the J-band used in the simulations, and the diagonal dashed line indicates the plasmon resonances. Both lines correspond to the position of the modes obtained from the model in the absence of electromagnetic coupling. The solid red lines indicate the simple prediction of the energy of the modes using eq 1 with the same value of $|g|/\kappa$.

presence of the J-aggregates. We focus on the other two maxima at longer wavelengths, which correspond to the two hybridized modes (UR and LR).

The top spectrum in Figure 2b corresponds to the hybrid structure for the smaller detuning, which is as small as ∼10 nm (estimated from the experimental spectra) and shows a clear double-peak structure, with the energy separating the UR and LR peaks estimated to be 265 meV. The two peaks remain visible and red shift as the detuning increases, with much stronger shifts for the LR resonance so that the total spectral separation becomes larger. The separation reaches 710 meV for the largest detuning achieved in our experiments (lowest line in Figure 2b).

The evolution of the energy of the two branches as obtained from the extinction measurements is summarized in Figure 3, where we have approximately subtracted the influence of the peak at ∼520 nm when extracting the peak position of the UR branch. The exact UR wavelength depends on the details of this procedure, and we estimate that a relatively small error of a few nanometers could be introduced for the most difficult case, which corresponds to the weakest detunings. Nonetheless, subtracting the ∼520 nm band is convenient when comparing the peak positions from experiments with those from theory, as the latter only exhibits the maxima corresponding to the UR and LR branches. The results in Figure 3 are typical of an anticrossing behavior with Rabi splitting $\hbar\Omega_R \approx 200$ meV (see below the details of how to extract the value for the Rabi splitting) as a result of the strong coupling of the J-band of the J-aggregates with the plasmon modes of the nanorods.

This value of splitting compares well with previous works studying strongly coupled hybrid systems formed by different silver and gold nanostructures combined with J-aggregates. To date the highest values of Rabi energies (up to 450 meV) have been reported for Ag/J-aggregates systems (Supporting Information S2). However, silver is known to suffer from rapid oxidation that strongly degrades plasmonic properties. Although Au-based plasmonic structures are much more photochemically stable, Au/J-aggregates systems have shown smaller values of Rabi splitting (up to 260 meV) (Supporting Information S1). Nevertheless the reported values as well as the Rabi splitting obtained in our experiments are of the same magnitude as the largest splittings observed in extended planar organic microcavities.[45,46]

The accurate determination of the Rabi splitting $\hbar\Omega_R$, defined as $\hbar\Omega_R = Re(E_+ - E_-)$ for $\delta = 0$, requires the exact values of $E_\pm$ (eq 1). This aspect is crucial to make a proper comparison with experimental data and to unambiguously identify the emergence of strong coupling; however, this estimation is often challenging because the positions of the experimental maxima do not exactly correspond to the values of $E_\pm$. This situation is clearly a challenge, for example, in the case of plasmonic systems with spectral Fano-like dips,[47,48] where destructive interference between two weakly coupled modes can lead to the emergence of two peaks without real mode splitting.

We use next a theoretical model to better identify the emergence of strong coupling in our system. The extinction can be addressed by classical models;[49,50] however, we use a quantum approach that allows us to model both the extinction and fluorescence, with a straightforward interpretation of the different parameters involved. Specifically, we model the plexcitonic structures through the Jaynes−Cumming Hamiltonian as a two-level system coupled to a quantized mode of a plasmonic cavity.[51−53] The illumination is considered at this

DOI: 10.1021/acs.jpclett.5b02512
J. Phys. Chem. Lett. 2016, 7, 354−362

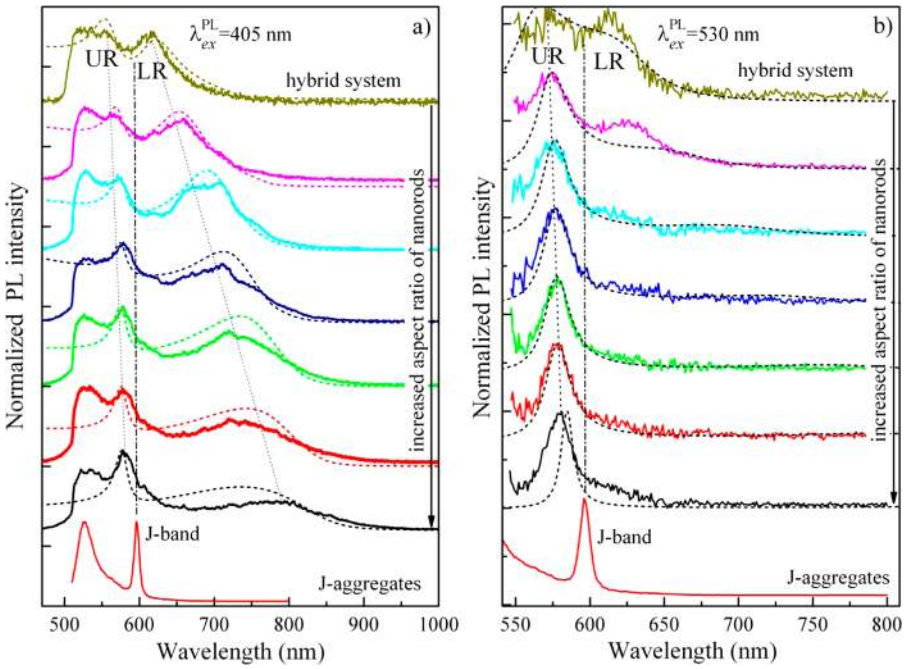

Figure 4. Normalized PL spectra (top seven solid lines) of the hybrid system formed by nanorods of different aspect ratios and J-aggregates, measured when using excitation at 405 (a) and 530 nm (b), in comparison with the PL spectra of pure J-aggregates measured in the absence of nanorods (bottom red curves). The upper spectra correspond to the smaller detuning (i.e., aspect ratio of nanorods is increased from top to bottom). Dashed curves are the normalized results of the theoretical calculations for $g/\kappa = -0.4i$, which assume incoherent excitation of (a) the plasmon mode or (b) the J-band transition. Vertical dashed-dotted line indicates the spectral position of the J-band, and thin dotted diagonal lines are just guides to the eye.

stage to be a classical plane wave of weak intensity I_0. The losses κ and resonant energy of the plasmon for each spectrum are obtained from measurements of the pristine plasmonic structures. The pure dephasing γ_d and energy of the J-aggregates are chosen to match the experimental results and remain the same for all the calculations, taking reasonable values when considering the spectra of the isolated J-aggregates. The spontaneous excitonic decay rate γ_s is assumed to be very small. The critical parameter in this model is the coupling strength g between the J-aggregate and the plasmon. We use a value of $g/\kappa = -0.4i$, which considerably exceeds the threshold $|g|/\kappa = 0.25$ that defines the onset of the strong coupling ($\hbar\Omega_R > 0$) for negligible molecular losses. The above condition for $\hbar\Omega_R > 0$ becomes $|g|/|\kappa - \gamma_s - 2\gamma_d| > 0.25$ if molecular losses are included. However, it has been pointed out that it might be more adequate to compare g with $\kappa + \gamma_s + 2\gamma_d$ to analyze the spectral separation between the peaks measured in experiments.[11] In our case, $\kappa \approx 10\gamma_d$, so that $|g|/|\kappa + \gamma_s + 2\gamma_d|$ remains larger than 0.25.

We also notice that the different parameters should in principle vary from individual rod to individual rod within each sample due to the inhomogeneous broadening caused, for example, by the size distribution of the nanorods. We adopt here the simpler option of using effective global values, and incorporate the effect of the inhomogenous broadening in the loss parameter κ, which is directly extracted from the measured spectra. If we were to focus in individual rods, a smaller value of κ should be used and $|g|/\kappa$ could be appreciably larger. Our assumption thus gives the most conservative (weakest) $|g|/\kappa$, based on the linewidth of the measured spectra, and a larger value should be considered in the analysis of single-rod quantum plasmonic experiments. In summary, as the separate analysis of each individual rod is not necessary in ensemble measurements, we discuss $|g|/\kappa$ in terms of the linewidth κ of the spectra as measured for the ensemble of pure rods. The detailed description of the Jaynes−Cummings Hamiltonian used and the value of the different parameters assumed are found in the Supporting Information S6.

The predictions of the model are compared with the normalized experimental results in Figure 2b, showing very good agreement for both the UR and LR peaks for all nanorods samples with different sizes. The agreement is emphasized in Figure 3, where we compare the position of the theoretical peaks for $g/\kappa = -0.4i$ (red circles) with the experimental values (blue squares). The solid red lines correspond to the theoretical position of the modes as obtained from eq 1, with $g/\kappa = -0.4i$. Both theoretical estimations do not superimpose because one (lines) accounts for the energy of the actual modes, whereas the other (symbols) considers the maximum of the peaks. Furthermore, when evaluating eq 1 we do not take into account that κ is not identical for all samples but rather use an average value. From eq 1 we can also estimate the Rabi energy at zero detuning $\delta = 0$, obtaining $\hbar\Omega_R \approx 200$ meV for $g/\kappa = -0.4i$. This value is in general agreement with our simple estimation from the position of the experimental peaks, but the more complete theoretical model has the advantage that it allows us to extract the mode energy (the quantity used in the definition of Ω_R) from the peak positions (obtained from the measurements). The anticrossing for a slightly larger value of $g/\kappa = -0.5i$ is shown in Supporting Information S9.

Next, we study the less understood influence of strong coupling between excitons and plasmon on the photoluminescence. The PL of plexitonic complexes identical to those in Figure 2 was measured using continuous excitation at wavelength λ_{ex}^{PL} = 405 nm (Figure 4a) and λ_{ex}^{PL} = 530 nm (Figure 4b). The red line at the bottom of both panels is the

DOI: 10.1021/acs.jpclett.5b02512
J. Phys. Chem. Lett. 2016, 7, 354−362

emission from the pure J-aggregates, which consists of a well-defined J-band centered at 600 nm (fwhm = 8.2 nm) and a monomeric peak with a maximum at 525 nm. In the following analysis we ignore the contribution of the latter and of the TM plasmon resonance (signal at wavelengths below ∼550 nm, which was cut off using a proper filter) because they do not affect the coupling with the exciton emitting at ∼600 nm.

For the smallest detuning δ (∼10 meV) between the plasmonic resonance of the gold nanorods and the extinction band of the J-aggregates, the PL spectrum of the hybrid system shows two peaks (Figure 4, upper curves for both excitation wavelengths). The spectral position of these two peaks is close to the spectral positions of the two (UR and LR) resonances in the extinction spectrum of the hybrid structure (Figure 2), although the spectral distance between the two PL peaks is slightly smaller, on the order of 230−240 meV for excitation at wavelength λ_{ex}^{PL} = 405 nm (Figure 4a) and 140−150 meV for λ_{ex}^{PL} = 530 nm (Figure 4b). The exact value is difficult to determine precisely in Figure 4b because of the experimental noise.

The observation of the emission from both the UR and LR in the spectra of the plexitonic nanosystem at room temperature is of particular interest because it enables the investigation of the recombination from both UR and LR states of the strongly coupled plexitonic system as well as the analysis of the energy-transfer dynamics between UR and LR states. Notably, it has been reported that the high energy state usually does not emit at room temperature due to an efficient population transfer to other excitonic states of the J-aggregates that are not coupled to plasmonic excitations.[11,36,42,54] The presence of these uncoupled emitters can be detected by the observation of a residual absorbance (or luminescence) peak at the wavelength of the J-band.[55,56] In our experiments, the excess of J-aggregates was separated from the hybrid nanostructures by centrifugation and redispersion of the plexitonic structures in water in a multistep manner. At each step the process was monitored by measuring the extinction spectra until the residual peak at the wavelength of the excitonic J-band completely disappeared, indicating a strongly decreased amount of unbound J-aggregates. The actual absence of unbound excitonic states would explain the suppression of the relaxation of the population toward uncoupled excitonic states (particularly at the smallest detunings). This procedure, together with the strongly enhanced emission from the hybridized J-band due to the coupling, can explain why measuring the radiative recombination from the UR branch becomes possible in our experiment.

The evolution of the spectra with increasing detuning depends on the excitation wavelength. The contribution from the UR at larger energies appears in all spectra and for both illuminations, becoming more clear as the detuning grows, and for excitation at 530 nm. For this excitation (Figure 4b), the lower energy LR peak vanishes very rapidly with increasing detuning, and it is only clearly observable for the two nanorod samples of smaller aspect ratios. The corresponding shift between these two cases (two upper spectra) is rather weak. For excitation at 405 nm (Figure 4a), a contribution from the two branches is observed for all detunings, and the shift of the LR peak, when comparing the two rods of smaller aspect ratio, is larger than for illumination at 530 nm. Nonetheless, as appreciated for large detuning, the LR shifts for excitation at 405 nm remain weaker than the shifts of the corresponding extinction peaks. As discussed later and in the Supporting Information, this is mostly due to the PL emission being less efficient at lower energies and not to a different δ.

We can gain additional insight into the experimental results by tracking the signal as a function of emission wavelength λ_{em}^{PL} in a model calculation. We use the same Jaynes−Cummings Hamiltonian as previously used for the estimation of the extinction, but we consider now a continuous incoherent pumping, as the coherence is lost in the luminescence process. To reproduce the experimental results, it is convenient to consider pumping of either the longitudinal dipolar plasmonic mode when modeling the excitation at λ_{em}^{PL} = 405 nm (Figure 4a) or the two-level J-aggregate excitation transition when reproducing the measurements with λ_{em}^{PL} = 530 nm illumination (Figure 4b). These choices are equivalent to arguing that, at the higher illumination energy, PL processes due to the plasmon excitation[57−60] are more efficient than those connected with the decay from higher energy states of the J-aggregates and vice versa at the lower energies.

The emission spectra are then obtained following the analytical approach introduced by Laussy et al.[41] and checked against numerical calculations. Notably, we use very similar parameters for the calculation of the luminescence as those used for the extinction, with only small differences in the values of (ω_{pl}, κ) characterizing the plasmon, as these are consistently extracted from the measurements of pristine rods for each set of spectra, as obtained before adding the J-aggregate. When treating the case of incoherent pumping of the plasmons, we rescale the results obtained directly from the model by a function $F(\lambda_{em}^{PL})$ obtained from the experimental spectra of the uncoupled pristine rods (see Supporting Information S6 and S7) and add a simple background $B(\lambda_{em}^{PL})$. The $F(\lambda_{em}^{PL})$ function in the model introduces the energy dependence of the PL process in metallic samples[57,59,61] as well as other effects such as the wavelength-dependence of dipolar emission. For the largest detunings, δ, the uncertainty introduced by $F(\lambda_{em}^{PL})$ can be comparable to the coupling-induced shifts; therefore, it is convenient in this case to focus on the results for the shorter rods. We discuss this model in more detail in the Supporting Information S6−S8.

We find a good agreement between the experiments and the model theory when comparing the normalized spectra for $g/\kappa = -0.4i$ with the PL spectra for both excitations λ_{ex}^{PL} (Figure 4a,b). The difference in the energies of the two resonant hybridized peaks for the smallest detuning δ is ∼250 meV for pumping of the longitudinal plasmon mode and roughly 150 meV for pumping of the exciton transition. (For the latter, the LR peak appears as a shoulder but becomes better defined if we increase g/κ.) Furthermore, as the detuning increases, the two peaks for λ_{ex}^{PL} = 405 nm (Figure 4a) and the UR resonance for λ_{ex}^{PL} = 530 nm (Figure 4b) remain visible and evolve in a similar manner both for the calculations and experiments. In contrast, the strength of the LR peak for λ_{ex}^{PL} = 530 nm decays very fast with increasing detuning, in agreement with the measurements. This would be due to the inefficient energy transfer from the more hybrid-like mode at larger energy to the plasmon-like resonance, when exciting the system via PL processes in the J-aggregate. This decay of the modal strength as the detuning increases is slightly faster in the theory, which may be related to the contribution in the experiments from rods of lower aspect ratio, rods uncoupled to J-aggregates, or incoherent excitation of the exciton.

In summary, we have shown that integration of gold nanorods with J-aggregates of a cyanine dye leads to a strong

DOI: 10.1021/acs.jpclett.5b02512
J. Phys. Chem. Lett. 2016, 7, 354−362

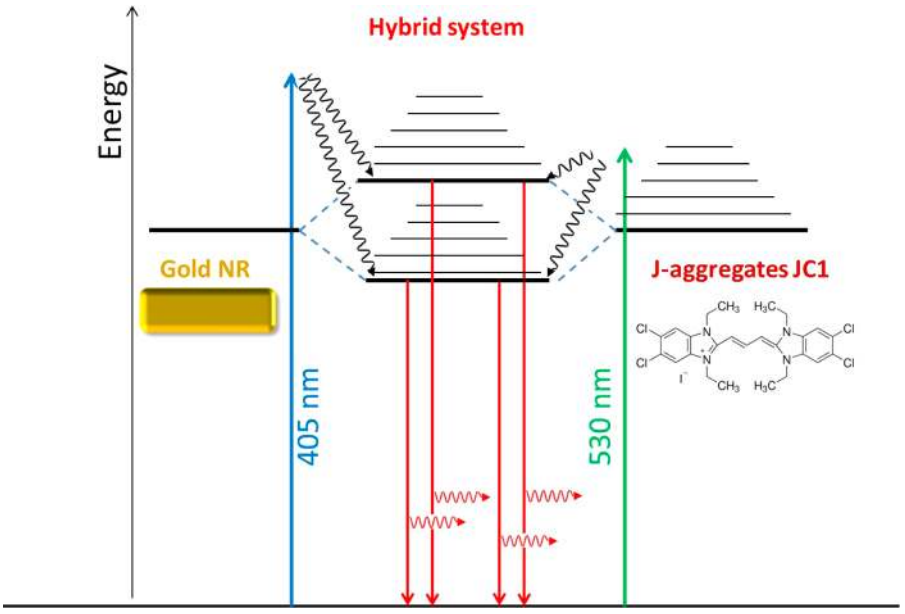

Figure 5. Scheme illustrating the proposed photoluminescence mechanism as a function of excitation wavelength for the hybrid system formed by nanorods and J-aggregates. The strong coupling between the plasmon mode (single level to the left) in the nanorods and the exciton in the J-aggregate (single level with vibronic structure to the right) leads to two hybridized modes (double level structure with vibronic states in the center). When the rod resonance and the J-band appear at a similar energy (low detuning), both hybrid modes can be excited incoherently via either the decay processes in the metal for 405 nm excitation (blue arrow) or nonradiative recombination in the J-aggregates when illuminating at 530 nm (green arrow). For large detuning, one of the hybrid modes is essentially plasmon-like and the other is exciton-like, and the illumination strongly affects their relative weight, with 530 nm light exciting preferentially the latter and 405 nm a more mixed balance. Black arrows show the relaxation channels of the excitation and red arrows indicate radiative recombination pathways. The narrower horizontal lines indicate vibrational or similar levels, which are indicated for completeness but do not need to be included in the theoretical model to reproduce the experimental result.

plexitonic coupling, observed as a double-peaked feature in the extinction and PL spectra. In the resonant regime, the Rabi splitting was estimated to be ∼200 meV, which is among the highest values reported to date for similar systems. The corresponding value of $|g|/\kappa$ is ∼0.4 when using the κ extracted from the measured extinction spectra of an inhomogeneous assembly or rods and should be larger for single rods. Moreover, the pronounced PL emission from both lower- and upper-energy states has allowed us to identify and study the influence of strong coupling on the PL spectra for two different excitation wavelengths. The results for both of these are similar in the case of weak detuning and indicative of Rabi splitting in fluorescence; however, as the detuning increases, we obtain a more clear evolution of the anticrossing when exciting at an energy significantly larger than the transition of the J-aggregate. We explain the difference as a consequence of predominantly pumping the plasmonic mode for the smaller incident wavelength λ_{ex}^{PL}, or the J-aggregate electronic transitions for the larger λ_{ex}^{PL} (see schematics of the processes in Figure 5). The PL model also suggests a value of $|g|/\kappa$ around 0.4, consistent with the value for the extinction, thus indicating the onset of the strong coupling.

Notably, by assuming a consistent strong coupling in equally prepared systems, the theoretical model can explain well the observed spectral behavior in both extinction and photoluminescence. Nonetheless, the experimental situation is significantly more complicated, and a more sophisticated model could include the right distribution of rod sizes and different degrees of J-aggregates coverage as well as provide a more accurate description of the PL process in gold and the complex electronic structure of the aggregate (with many possible paths of energy transfer). Including this complexity could explain the remaining differences between theory and experiments and also give a more physical understanding of the background $B(\lambda_{em}^{PL})$, introduce the efficiency of the PL emission ($F(\lambda_{em}^{PL})$ factor) in a more rigorous manner, and allow us to better understand under which conditions the incoherent pumping of the plasmon mode or of the J-aggregate dominates the PL signal.

Our results thus support that the anticrossing behavior typical of the strong coupling regime can be observed in our plexitonic system at room temperature not only in the extinction but also in the PL spectra. These findings could open a new avenue toward the development of novel light-emitting nanostructures with strong exciton−plasmon interaction.

METHODS

Chemicals. Cyanine dye 5,5′,6,6′-tetrachloro-1,1′,3,3′-tetraethylimidacarbocyanine iodide (JC1), tetrachloroauric acid ($HAuCl_4$), sodium borohydride ($NaBH_4$) hexadecyltrimethylammonium bromide (CTAB), silver nitrate ($AgNO_3$), hydrochloric acid (HCl), and ascorbic acid (AA) were purchased from Sigma-Aldrich. Chemical structure of JC1 is shown in Supporting Information (S5).

Formation of J-Aggregates. J-aggregates were formed using JC1 cyanine. This dye has low aqueous solubility and forms J-aggregates spontaneously upon dissolution of this dye in water at pH 8.[20,62]

Synthesis and Oxidation of Nanorods. 1.38, 1.25, 1.10, 0.85, 0.50, and 0.30 mL of Au^{+3}-CTAB complex ([Au] = 1 mM, [CTAB] = 100 mM) was added dropwise (0.1 mL/min) and under magnetic stirring to six different vials, each containing 10 mL of initially synthesized gold nanorods[43] and labeled a−f,

DOI: 10.1021/acs.jpclett.5b02512
J. Phys. Chem. Lett. 2016, 7, 354−362

respectively. Each solution was allowed to react at 30 °C for 1 h. Subsequently, the solutions were centrifuged twice (6000−9000 rpm, 40 min) to remove excess gold salt and redispersed in CTAB solution (2.5 mL, 15 mM).

Formation of the Hybrid Structures. Hybrid structures of gold nanorods and J-aggregates were produced by the addition of 10 μL of concentrated ethanol solution of JC1 dye to 1 mL of an aqueous solution of gold nanorods in the presence of ammonia at pH 8, followed by gentle stirring for 15 min. To separate hybrid structures (i.e., J-aggregates bound to nanorods) from monomer dye molecules and J-aggregates, which did not bound to gold nanorods, we centrifuged the solution at 3800 rpm for 2 min, and it was redispersed in aqueous solution.

Optical Characterization. All experiments were performed in an ambient atmosphere at room temperature. Doubly purified deionized water from an 18 MU Millipore system was used for all dilutions. The optical extinction spectra were measured using a Cary 50 spectrometer (Agilent Technologies).

Photoluminescence spectra of bare gold nanorods and hybrid structures of gold nanorods and J-aggregates with laser excitation at 405 nm were recorded using Olympus IX71 inverted confocal microscope system equipped with Ocean Optics QEPro high-performance spectrometer. The PL spectra with wavelength of excitation 530 nm were measured using a Cary Eclipse spectrophotometer (Agilent Technologies).

Raman scattering (SERS) measurements were carried out using a confocal Raman microscopy setup (Alpha300, 600 mm^{-1} grating, 3 cm^{-1} spectral resolution, continuous wave laser excitation at 532 nm, WITec).

A transmission electron microscopy (TEM) image of nanorods was obtained using transmission electron microscopy system FEG-TEM of type JEOL JEM-2100F UHR.

■ ASSOCIATED CONTENT

Supporting Information

The Supporting Information is available free of charge on the ACS Publications website at DOI: 10.1021/acs.jpclett.5b02512.

Rabi splitting energies reported to date in Au/J-aggregates and Ag/J-aggregates-based hybrid nanostructures. Aspect ratios and of nanorods samples and corresponding extinction spectra of gold nanorods. Chemical structure of JC1. Description of the theoretical model used and discussion on the effect on the calculated signal due to the scaling function $F(\lambda_{em}^{PL})$ and the background added. Comparison of the theoretical results for two different coupling strengths. (PDF)

■ AUTHOR INFORMATION

Corresponding Authors

*Y.P.R.: E-mail: yury.rakovich@ehu.eus.

*R.E.: E-mail: ruben_esteban@ehu.eus.

Author Contributions

The manuscript was written through contributions of all authors. All authors have given approval to the final version of the manuscript.

Notes

The authors declare no competing financial interest.

■ ACKNOWLEDGMENTS

We acknowledge financial support from Projects FIS2013-41184-P and MAT2013-46101-R of the Spanish Ministry of Economy and Competitiveness (MINECO) and ETORTEK project NANOGUNE'14. R.E. acknowledges funding as Fellow Gipuzkoa of the Gipuzkoako Foru Aldundia through Feder Funds of the European Union "Una manera de hacer Europa". We acknowledge helpful discussions with Kai-Qiang Lin and Bin Ren.

■ REFERENCES

(1) Fofang, N. T.; Park, T.-H.; Neumann, O.; Mirin, N. A.; Nordlander, P.; Halas, N. J. Plexcitonic Nanoparticles: Plasmon-Exciton Coupling in Nanoshell-J-Aggregate Complexes. *Nano Lett.* **2008**, *8*, 3481−3487.

(2) Ni, W.; Ambjörnsson, T.; Apell, S. P.; Chen, H.; Wang, J. Observing Plasmonic-Molecular Resonance Coupling on Single Gold Nanorods. *Nano Lett.* **2010**, *10*, 77−84.

(3) Wiederrecht, G. P.; Wurtz, G. A.; Hranisavljevic, J. Coherent Coupling of Molecular Excitons to Electronic Polarizations of Noble Metal Nanoparticles. *Nano Lett.* **2004**, *4*, 2121−2125.

(4) Chen, H.; Ming, T.; Zhao, L.; Wang, F.; Sun, L.-D.; Wang, J.; Yan, C.-H. Plasmon−molecule interactions. *Nano Today* **2010**, *5*, 494−505.

(5) Wiederrecht, G. P.; Wurtz, G. A.; Bouhelier, A. Ultrafast hybrid plasmonics. *Chem. Phys. Lett.* **2008**, *461*, 171−179.

(6) Zheng, Y. B.; Kiraly, B.; Weiss, P. S.; Huang, T. J. Molecular plasmonics for biology and nanomedicine. *Nanomedicine* **2012**, *7*, 751−770.

(7) Wiederrecht, G. P.; Hall, J. E.; Bouhelier, A. Control of Molecular Energy Redistribution Pathways via Surface Plasmon Gating. *Phys. Rev. Lett.* **2007**, *98*, 083001.

(8) Dong, Z. C.; Zhang, X. L.; Gao, H. Y.; Luo, Y.; Zhang, C.; Chen, L. G.; Zhang, R.; Tao, X.; Zhang, Y.; Yang, J. L.; Hou, J. G. Generation of molecular hot electroluminescence by resonant nanocavity plasmons. *Nat. Photonics* **2010**, *4*, 50−54.

(9) Hennessy, K.; Badolato, A.; Winger, M.; Gerace, D.; Atatüre, M.; Gulde, S.; Fält, S.; Hu, E. L.; Imamoglu, A. Quantum nature of a strongly coupled single quantum dot-cavity system. *Nature* **2007**, *445*, 896−899.

(10) Auffèves, A.; Gérard, J.-M.; Poizat, J.-P. Pure emitter dephasing: A resource for advanced solid-state single-photon sources. *Phys. Rev. A: At., Mol., Opt. Phys.* **2009**, *79*, 053838.

(11) Törmä, P.; Barnes, W. L. Strong coupling between surface plasmon polaritons and emitters: a review. *Rep. Prog. Phys.* **2015**, *78*, 013901.

(12) Vasa, P.; Wang, W.; Pomraenke, R.; Lammers, M.; Maiuri, M.; Manzoni, C.; Cerullo, G.; Lienau, L. Real-time observation of ultrafast Rabi oscillations between excitons and plasmons in metal nanostructures with J-aggregates. *Nat. Photonics* **2013**, *7*, 128−132.

(13) Wang, W.; Vasa, P.; Sommer, E.; De Sio, A.; Gross, P.; Vogelgesang, R.; Lienau, C. Observation of Lorentzian lineshapes in the room temperature optical spectra of strongly coupled Jaggregate/metal hybrid nanostructures by linear two-dimensional optical spectroscopy. *J. Opt.* **2014**, *16*, 114021.

(14) Trügler, A.; Hohenester, U. Strong coupling between a metallic nanoparticle and a single molecule. *Phys. Rev. B: Condens. Matter Mater. Phys.* **2008**, *77*, 115403.

(15) Savasta, S.; Saija, R.; Ridolfo, A.; Di Stefano, O.; Denti, P.; Borghese, F. Nanopolaritons: Vacuum Rabi Splitting with a Single Quantum Dot in the Center of a Dimer Nanoantenna. *ACS Nano* **2010**, *4*, 6369−6376.

(16) Hümmer, T.; García-Vidal, F. J.; Martín-Moreno, L.; Zueco, D. Weak and strong coupling regimes in plasmonic QED. *Phys. Rev. B: Condens. Matter Mater. Phys.* **2013**, *87*, 115419.

(17) Wurthner, F.; Kaiser, T. E.; Saha-Moller, C. R. J-Aggregates: From Serendipitous Discovery to Supramolecular Engineering of Functional Dye Materials. *Angew. Chem., Int. Ed.* **2011**, *50*, 3376−3410.

(18) Hakala, T. K.; Toppari, J. J.; Kuzyk, A.; Pettersson, M.; Tikkanen, H.; Kunttu, H.; Torma, P. Vacuum Rabi Splitting and

DOI: 10.1021/acs.jpclett.5b02512
J. Phys. Chem. Lett. 2016, 7, 354−362

Strong-Coupling Dynamics for Surface-Plasmon Polaritons and Rhodamine 6G Molecules. *Phys. Rev. Lett.* **2009**, *103*, 053602−4.
(19) Chantharasupawong, P.; Tetard, L.; Thomas, J. Coupling Enhancement and Giant Rabi-Splitting in Large Arrays of Tunable Plexcitonic Substrates. *J. Phys. Chem. C* **2014**, *118*, 23954−23962.
(20) Melnikau, D.; Savateeva, D.; Susha, A. S.; Rogach, A. L.; Rakovich, Y. P. Strong plasmon-exciton coupling in a hybrid system of gold nanostars and J-aggregates. *Nanoscale Res. Lett.* **2013**, *8*, 134−6.
(21) Zheng, Y. B.; Juluri, B. K.; Lin Jensen, L.; Ahmed, D.; Lu, M.; Jensen, L.; Huang, T. J. Dynamic Tuning of Plasmon−Exciton Coupling in Arrays of Nanodisk−J-aggregate Complexes. *Adv. Mater.* **2010**, *22*, 3603−3607.
(22) Sugawara, Y.; Kelf, T. A.; Baumberg, J. J.; Abdelsalam, M. E.; Bartlett, P. N. Strong Coupling between Localized Plasmons and Organic Excitons in Metal Nanovoids. *Phys. Rev. Lett.* **2006**, *97*, 266808.
(23) Schlather, A. E.; Large, N.; Urban, A. S.; Nordlander, P.; Halas, N. J. Near-Field Mediated Plexcitonic Coupling and Giant Rabi Splitting in Individual Metallic Dimers. *Nano Lett.* **2013**, *13*, 3281−3286.
(24) Lekeufack, D. D.; Brioude, A.; Coleman, A. W.; Miele, P.; Bellessa, J.; De Zeng, L.; Stadelmann, P. Core-shell gold J-aggregate nanoparticles for highly efficient strong coupling applications. *Appl. Phys. Lett.* **2010**, *96*, 253107.
(25) Wurtz, G. A.; Evans, P. R.; Hendren, W.; Atkinson, R.; Dickson, W.; Pollard, R. J.; Harrison, W.; Bower, C.; Zayats, A. V. Molecular Plasmonics with Tunable Exciton-Plasmon Coupling Strength in J-Aggregate Hybridized Au Nanorod Assemblies. *Nano Lett.* **2007**, *7*, 1297−1303.
(26) Vasa, P.; Pomraenke, R.; Cirmi, G.; De Re, E.; Wang, W.; Schwieger, S.; Leipold, D.; Runge, E.; Cerullo, G.; Lienau, C. Ultrafast Manipulation of Strong Coupling in Metal−Molecular Aggregate Hybrid Nanostructures. *ACS Nano* **2010**, *4*, 7559−7565.
(27) Bellessa, J.; Symonds, C.; Vynck, K.; Lemaitre, A.; Brioude, A.; Beaur, L.; Plenet, J. C.; Viste, P.; Felbacq, D.; Cambril, E.; Valvin, P. Giant Rabi splitting between localized mixed plasmon-exciton states in a two-dimensional array of nanosize metallic disks in an organic semiconductor. *Phys. Rev. B: Condens. Matter Mater. Phys.* **2009**, *80*, 033303.
(28) Salomon, A.; Wang, S.; Hutchison, J. A.; Genet, C.; Ebbesen, T. W. Strong Light-Molecule Coupling on Plasmonic Arrays of Different Symmetry. *ChemPhysChem* **2013**, *14*, 1882−1886.
(29) Balci, S. Ultrastrong plasmon-exciton coupling in metal nanoprisms with J-aggregates. *Opt. Lett.* **2013**, *38*, 4498−4501.
(30) Symonds, C.; Bonnand, C.; Plenet, J. C.; Bréhier, A.; Parashkov, R.; Lauret, J. S.; Deleporte, E.; Bellessa, J. Particularities of surface plasmon−exciton strong coupling with large Rabi splitting. *New J. Phys.* **2008**, *10*, 065017.
(31) Aberra Guebrou, S.; Symonds, C.; Homeyer, E.; Plenet, J. C.; Gartstein, Y. N.; Agranovich, V. M.; Bellessa, J. Coherent Emission from a Disordered Organic Semiconductor Induced by Strong Coupling with Surface Plasmons. *Phys. Rev. Lett.* **2012**, *108*, 066401.
(32) Bonnand, C.; Bellessa, J.; Plenet, J. C. Properties of surface plasmons strongly coupled to excitons in an organic semiconductor near a metallic surface. *Phys. Rev. B: Condens. Matter Mater. Phys.* **2006**, *73*, 245330.
(33) Zengin, G.; Wersall, M.; Nilsson, S.; Antosiewicz, T. A.; Kall, M.; Shegai, T. Realizing strong light-matter interactions between single nanoparticle plasmons and molecular excitons at ambient conditions. *Phys. Rev. Lett.* **2015**, *114*, 157401.
(34) Dintinger, J.; Klein, S.; Bustos, F.; Barnes, W. L.; Ebbesen, T. W. Strong coupling between surface plasmon-polaritons and organic molecules in subwavelength hole arrays. *Phys. Rev. B: Condens. Matter Mater. Phys.* **2005**, *71*, 035424.
(35) DeLacy, B. G.; Miller, O. D.; Hsu, C. W.; Zander, Z.; Lacey, S.; Yagloski, R.; Fountain, A. W.; Valdes, E.; Anquillare, E.; Soljačić, M.; Johnson, S. G.; Joannopoulos, J. D. Coherent Plasmon-Exciton Coupling in Silver Platelet-J-aggregate Nanocomposites. *Nano Lett.* **2015**, *15*, 2588−2593.
(36) Bellessa, J.; Bonnand, C.; Plenet, J. C.; Mugnier, J. Strong Coupling between Surface Plasmons and Excitons in an Organic Semiconductor. *Phys. Rev. Lett.* **2004**, *93*, 036404.
(37) Bonnand, C.; Bellessa, J.; Symonds, C.; Plenet, J. C. Polaritonic emission via surface plasmon cross coupling. *Appl. Phys. Lett.* **2006**, *89*, 231119.
(38) Balci, S.; Kocabas, C.; Ates, S.; Karademir, E.; Salihoglu, O.; Aydinli, A. Tuning surface plasmon-exciton coupling via thickness dependent plasmon damping. *Phys. Rev. B: Condens. Matter Mater. Phys.* **2012**, *86*, 235402.
(39) Zengin, G.; Johansson, G.; Johansson, P.; Antosiewicz, T. J.; Käll, M.; Shegai, T. Approaching the strong coupling limit in single plasmonic nanorods interacting with J-aggregates. *Sci. Rep.* **2013**, *3*, 3074.
(40) Rudin, S.; Reinecke, T. L. Oscillator model for vacuum Rabi splitting in microcavities. *Phys. Rev. B: Condens. Matter Mater. Phys.* **1999**, *59*, 10227−10233.
(41) Laussy, F. P.; del Valle, E.; Tejedor, C. Luminescence spectra of quantum dots in microcavities. I. Bosons. *Phys. Rev. B: Condens. Matter Mater. Phys.* **2009**, *79*, 235325.
(42) Agranovich, V. M.; Litinskaia, M.; Lidzey, D. G. Cavity polaritons in microcavities containing disordered organic semiconductors. *Phys. Rev. B: Condens. Matter Mater. Phys.* **2003**, *67*, 085311.
(43) Liu, M.; Guyot-Sionnest, P. Mechanism of Silver(I)-Assisted Growth of Gold Nanorods and Bipyramids. *J. Phys. Chem. B* **2005**, *109*, 22192−22200.
(44) Rodríguez-Fernández, J.; Pérez-Juste, J.; Mulvaney, P.; Liz-Marzán, L. M. Spatially-Directed Oxidation of Gold Nanoparticles by Au(III)−CTAB Complexes. *J. Phys. Chem. B* **2005**, *109*, 14257−14261.
(45) Tischler, J. R.; Bradley, M. S.; Zhang, Q.; Atay, T.; Nurmikko, A.; Bulovic, V. Solid state cavity QED: Strong coupling in organic thin films. *Org. Electron.* **2007**, *8*, 94−113.
(46) Pirotta, S.; Patrini, M.; Liscidini, M.; Galli, M.; Dacarro, G.; Canazza, G.; Guizzetti, G.; Comoretto, D.; Bajoni, D. Strong coupling between excitons in organic semiconductors and Bloch surface waves. *Appl. Phys. Lett.* **2014**, *104*, 051111.
(47) Artuso, R. D.; Bryant, G. W. Optical Response of Strongly Coupled Quantum Dot-Metal Nanoparticle Systems: Double Peaked Fano Structure and Bistability. *Nano Lett.* **2008**, *8*, 2106−2111.
(48) Luk'yanchuk, B.; Zheludev, N. I.; Maier, S. A.; Halas, N. J.; Nordlander, P.; Giessen, H.; Chong, C. T. The Fano resonance in plasmonic nanostructures and metamaterials. *Nat. Mater.* **2010**, *9*, 707−715.
(49) Pérez-González, O.; Zabala, N.; Aizpurua, J. Optical properties and sensing in plexcitonic nanocavities: from simple molecular linkers to molecular aggregate layers. *Nanotechnology* **2014**, *25*, 035201.
(50) Antosiewicz, T. J.; Apell, S. P.; Shegai, T. Plasmon−Exciton Interactions in a Core−Shell Geometry: From Enhanced Absorption to Strong Coupling. *ACS Photonics* **2014**, *1*, 454−463.
(51) Savage, C. M. Quantum Optics with One Atom in an Optical Cavity. *J. Mod. Opt.* **1990**, *37*, 1711−1725.
(52) Esteban, R.; Aizpurua, J.; Bryant, G. W. Strong coupling of single emitters interacting with phononic infrared antennae. *New J. Phys.* **2014**, *16*, 013052.
(53) Shore, B. W.; Knight, P. L. The Jaynes-Cummings Model. *J. Mod. Opt.* **1993**, *40*, 1195−1238.
(54) Lidzey, D. G.; Bradley, D. D. C.; Virgili, T.; Armitage, A.; Skolnick, M. S.; Walker, S. Room Temperature Polariton Emission from Strongly Coupled Organic Semiconductor Microcavities. *Phys. Rev. Lett.* **1999**, *82*, 3316−3319.
(55) Canaguier-Durand, A.; Devaux, E.; George, J.; Pang, Y.; Hutchison, J. A.; Schwartz, T.; Genet, C.; Wilhelms, N.; Lehn, J.-M.; Ebbesen, T. W. Thermodynamics of Molecules Strongly Coupled to the Vacuum Field. *Angew. Chem., Int. Ed.* **2013**, *52*, 10533−10536.
(56) Schwartz, T.; Hutchison, J. A.; Léonard, J.; Genet, C.; Haacke, S.; Ebbesen, T. W. Polariton Dynamics under Strong Light−Molecule Coupling. *ChemPhysChem* **2013**, *14*, 125−131.

DOI: 10.1021/acs.jpclett.5b02512
J. Phys. Chem. Lett. 2016, 7, 354−362

(57) Andersen, S. K. H.; Pors, A.; Bozhevolnyi, S. I. Gold Photoluminescence Wavelength and Polarization Engineering. *ACS Photonics* **2015**, *2*, 432−438.
(58) Dulkeith, E.; Niedereichholz, T.; Klar, T. A.; Feldmann, J.; von Plessen, G.; Gittins, D. I.; Mayya, K. S.; Caruso, F. Plasmon emission in photoexcited gold nanoparticles. *Phys. Rev. B: Condens. Matter Mater. Phys.* **2004**, *70*, 205424.
(59) Hu, H.; Duan, H.; Yang, J. K. W.; Shen, Z. X. Plasmon-Modulated Photoluminescence of Individual Gold Nanostructures. *ACS Nano* **2012**, *6*, 10147−10155.
(60) Hugall, J. T.; Baumberg, J. J. Demonstrating Photoluminescence from Au is Electronic Inelastic Light Scattering of a Plasmonic Metal: The Origin of SERS Backgrounds. *Nano Lett.* **2015**, *15*, 2600−2604.
(61) Lumdee, C.; Yun, B.; Kik, P. G. Gap-Plasmon Enhanced Gold Nanoparticle Photoluminescence. *ACS Photonics* **2014**, *1*, 1224−1230.
(62) Melnikau, D.; Savateeva, D.; Gun'ko, Y. K.; Rakovich, Y. P. Strong Enhancement of Circular Dichroism in a Hybrid Material Consisting of J-Aggregates and Silver Nanoparticles. *J. Phys. Chem. C* **2013**, *117*, 13708−13712.

DOI: 10.1021/acs.jpclett.5b02512
J. Phys. Chem. Lett. 2016, 7, 354−362